



## ■ TRAUMA: RESEARCH

# Effect of low-intensity pulsed ultrasound stimulation on callus remodelling in a gap-healing model

## EVALUATION BY BONE MORPHOMETRY USING THREE-DIMENSIONAL QUANTITATIVE MICRO-CT

K. Tobita,  
I. Ohnishi,  
T. Matsumoto,  
S. Ohashi,  
M. Bessho,  
M. Kaneko,  
J. Matsuyama,  
K. Nakamura

*From the University  
of Tokyo, Tokyo,  
Japan*

**We evaluated the effect of low-intensity pulsed ultrasound stimulation (LIPUS) on the remodelling of callus in a rabbit gap-healing model by bone morphometric analyses using three-dimensional quantitative micro-CT. A tibial osteotomy with a 2 mm gap was immobilised by rigid external fixation and LIPUS was applied using active translucent devices. A control group had sham inactive transducers applied. A region of interest of micro-CT was set at the centre of the osteotomy gap with a width of 1 mm. The morphometric parameters used for evaluation were the volume of mineralised callus (BV) and the volumetric bone mineral density of mineralised tissue (mBMD). The whole region of interest was measured and subdivided into three zones as follows: the periosteal callus zone (external), the medullary callus zone (endosteal) and the cortical gap zone (intercortical). The BV and mBMD were measured for each zone.**

**In the endosteal area, there was a significant increase in the density of newly formed callus which was subsequently diminished by bone resorption that overwhelmed bone formation in this area as the intramedullary canal was restored. In the intercortical area, LIPUS was considered to enhance bone formation throughout the period of observation. These findings indicate that LIPUS could shorten the time required for remodelling and enhance the mineralisation of callus.**

■ K. Tobita, MD, Orthopaedic Surgeon  
■ I. Ohnishi, MD, PhD, Assistant Professor  
■ T. Matsumoto, MD, Orthopaedic Surgeon  
■ S. Ohashi, MD, PhD, Orthopaedic Surgeon  
■ M. Bessho, MD, PhD, Orthopaedic Surgeon  
■ M. Kaneko, MD, Orthopaedic Surgeon  
■ J. Matsuyama, MD, Orthopaedic Surgeon  
■ K. Nakamura, MD, PhD, Professor  
Department of Orthopaedic Surgery, Faculty of Medicine University of Tokyo, 7-3-1 Hongo, Bunkyo-ku, Tokyo 113-0033, Japan.

Correspondence should be sent to Professor I. Ohnishi; e-mail: ohnishi-i@umin.ac.jp

©2011 British Editorial Society of Bone and Joint Surgery  
doi:10.1302/0301-620X.93B4.25449 \$2.00

*J Bone Joint Surg [Br]*  
2011;93-B:525-30.

Received 29 June 2010;  
Accepted after revision 6  
December 2010

The effects of low-intensity pulsed ultrasound stimulation (LIPUS) are reportedly derived from the promotion of cell differentiation, which induces acceleration of fracture healing with earlier restoration of strength.<sup>1</sup>

Previous studies have investigated which stages of healing are affected by LIPUS. Many have suggested that LIPUS affects the inflammation, angiogenesis and formation stages of soft callus.<sup>2-4</sup> However, whether it influences the formation of hard callus or remodelling remains unclear.<sup>1,5,6</sup> Most previous studies have investigated the effects of LIPUS by histological evaluation, which is limited to observation in a two-dimensional (2D) plane. Another method adopted has been mechanical testing of harvested specimens, but this is limited since testing is destructive and the strength of the healing site is evaluated in only one of many planes.<sup>7</sup>

In recent years, several studies have investigated the morphometry of the site of fracture healing using micro-CT.<sup>8-10</sup> The advantage of

this technique lies in its non-destructive morphological and densitometric assessments in a three-dimensional (3D) plane. However, evaluation by micro-CT of the effects of LIPUS is only possible after healing has progressed to mineralisation of the callus. This period comprises two stages: the modelling period, during which callus is formed, and the remodelling period, during which mineralised tissues are redistributed by the processes of formation and resorption to restore the original structure.<sup>11</sup> The effects of LIPUS should be evaluated in both of these stages. In the modelling period, callus is formed externally from the periosteum and endosteally from the endosteum. The subsequent remodelling period partly overlaps the modelling period. If LIPUS enhances fracture healing by shortening either one of these processes, morphometry by means of micro-CT could identify spatial changes in the localisation of callus in 3D planes. However, no quantitative studies have included 3D morphological evaluation using micro-CT.

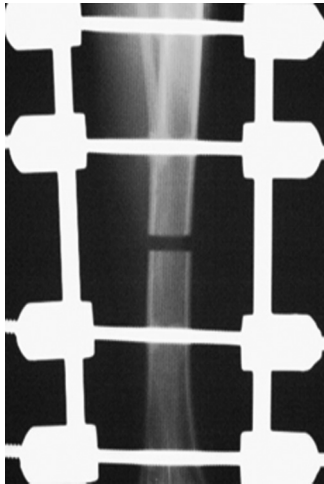


Fig. 1

Radiograph showing the osteotomy of the right tibia with a 2 mm gap between bone fragments rigidly stabilised by a four-pin, double-bar external fixator.

Our aim was to evaluate quantitatively the effect of LIPUS on bone healing by means of micro-CT throughout both modelling and remodelling using a gap-healing model in the rabbit.

## Materials and Methods

**Creation of the model.** We used 42 skeletally mature male Japanese white rabbits aged between 21 and 23 weeks and weighing between 3.4 kg and 4.0 kg (Kitayama Labs, Nagano, Japan). Under general anaesthesia, the right hind limb was prepared using a routine aseptic technique. Before the creation of an osteotomy four transfixion pins (diameter, 2 mm; length, 50 mm) were inserted at the metaphyseal regions of the tibia in the frontal plane using a custom-made driver. An anteromedial incision 2 cm in length was made, and the tibia exposed using two mini-retractors after elevating the periosteum. A transverse osteotomy was performed using an MDS36-30 T-saw (MANI, Tochigi, Japan) with a blade 0.36 mm thick in the mid-shaft of the tibia to produce a gap of 2 mm at 12 mm distal to the tibiofibular junction. The osteotomy was immobilised using the transfixion pins which were attached to an external fixator with KE double side bars (IMEX Veterinary Inc., Longview, Texas). The gap was confirmed by inserting a 2 mm spacer block. The site was thoroughly irrigated with saline to ensure that no tissue (bone, muscle, or fascia) was left in the gap. The soft tissues were then re-approximated, and the skin was closed. Proper alignment of the bone fragments was confirmed radiologically (Fig. 1). All the procedures were performed in accordance with the guidelines of the Association for Assessment and Accreditation of Laboratory Animal Care.

**LIPUS treatment.** We used the LIPUS model SAFHS 2000J (Teijin Pharma, Tokyo, Japan) which transmits a burst of 1.5 MHz sine waves of 200  $\mu$ sec repeated at 1 kHz with a mean intensity of 30m W/cm<sup>2</sup>.<sup>12,13</sup> After post-operative day 3, the LIPUS treatment was commenced under general anaesthesia for all animals. The animals were divided into two groups of seven rabbits, comprising a LIPUS and a control group. In the former group the transducer was placed on the anterior surface of the operated leg using ultrasound coupling gel for 20 minutes, six times per week for four, six or eight weeks. The control group had a sham inactive transducer applied which was used under exactly the same conditions as in the LIPUS group.

Experimental evaluations were conducted in a blinded manner and the animals were assigned to the two groups in a randomised manner using the envelope method. The same method was used to determine the duration of treatment.

**Post-operative management.** All the animals were allowed to move freely post-operatively in their cages bearing full weight. Subcutaneous buprenorphine (Otsuka Pharmaceutical, Tokyo, Japan) was injected for relief from pain. The environment was provided in accordance with the guidelines of the Institute of Laboratory Animal Resources and in compliance with the Guide for the Care and Use of Laboratory Animals. General conditions were checked for all the animals at least once a day. Food intake, activity and the condition of the scar were checked. Body-weight was measured on the day of operation and every two weeks. For post-operative care of the external fixator, we checked the clamps daily, and tightened the frame as necessary. The fixator was protected using gauze with a shock-absorbing material. In order to prevent infection at the pin site, irrigation of the pin sites was performed daily. There were no cases of fracture, infection or unexpected death.

**Radiography.** Anteroposterior radiographs of the tibia were taken together with a 2 mm incremental lead gauge under a tube voltage of 48 kV and current of 3.20 mAs immediately post-operatively and every two weeks thereafter to confirm the alignment of the osteotomy and to evaluate the size of the gap. Each radiograph was taken under exactly the same conditions using a standardised protocol. The gap was then measured by counting pixels overlying it using Photoshop CS3 software (Adobe Systems, San Jose, California). Pixel spacing of the digitised radiograph was calibrated by the number of pixels overlying each step of the lead gauge.

**Micro-CT.** The animals were killed after four, six and eight weeks and the right tibia was removed and scanned by micro-CT (ScanXmate-E090; Comscantecno, Kanagawa, Japan). The scan was performed along the long axis of the diaphysis, with a voltage of 60 kVp and a current of 80  $\mu$ A. The area of the scan was 5 mm proximal and 5 mm distal to the centre of the gap, with a resolution of voxel size of 28.57  $\mu$ m<sup>3</sup>. The region of interest (ROI) was set at the area of callus healing defined by the gap filled with callus in 2D-CT (Fig. 2) and extended 0.5 mm proximally and distally to the centre of the gap with a total of 36 CT axial scans. A 3D

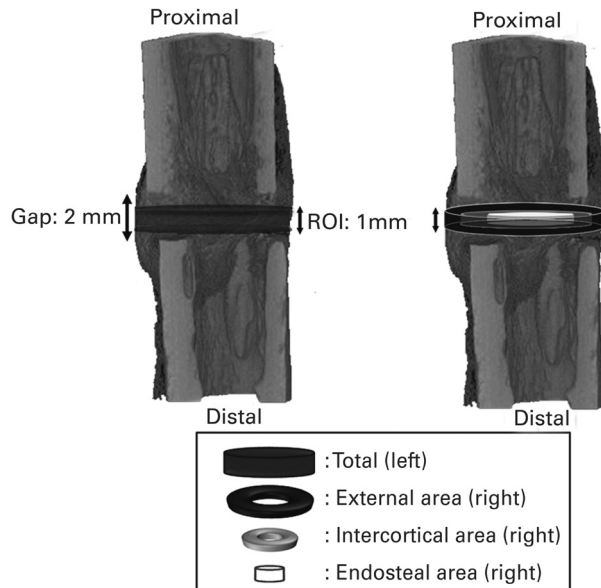


Fig. 2

The region of interest (ROI) was set at the callus healing area, defined as the centre of the osteotomy gap with a width of 1 mm (left). This area was subdivided into three zones: the periosteal callus zone (external, black zone in right); the medullary callus zone (endosteal, white zone in right); and the remaining area as the cortical gap zone (intercortical, grey zone in right).

reconstruction of mineralised tissue was performed using TRI-BONE software (Ratoc System Engineering, Tokyo, Japan). A threshold for newly formed mineralised callus was set at  $200 \text{ mg/cm}^3$ .<sup>14,15</sup> Morphometric parameters used for the evaluation were mineralised callus volume (BV,  $\text{cm}^3$ ) and mineralised callus content (BMC, mg) calculated from the contoured ROI in 3D images and volumetric bone mineral density of mineralised tissue comprising the callus (mBMD,  $\text{mBMD} = \text{BMC}/\text{BV}$ ,  $\text{mgHA}/\text{cm}^3$ ).<sup>9</sup> The ROI was subdivided into three zones (Fig. 2) as follows: a periosteal callus zone (external; black zone in Figure 2); a medullary callus zone (endosteal; white zone in Figure 2); and the cortical gap zone as the remaining zone (intercortical: grey zone in Figure 2). The area of the three zones was segmented with a least-squares geometrical algorithm using the micro-CT scans of cortices of the proximal and distal levels of the bone fragments at the gap. The outer surface of the proximal and distal ends close to the gap were extracted with a threshold of  $200 \text{ mg/cm}^3$  and divided by voxels with a size of  $28.57 \mu\text{m}^3$ . The co-ordinates of the centre of each voxel were then calculated using the TRI-BONE software.

After identifying corresponding sites between proximal and distal endpoints, a triangular patch was created with the line connecting these two corresponding points and the alignment of two corresponding voxels.<sup>16</sup> A surface model created by these patches interpolated the outer cortical surface at the gap. External callus was defined as the callus outside this surface. A surface model was also created from the inner surface of cortices of the proximal and distal ends

of the bone fragments at the gap by exactly the same procedure as was used to define external callus. Endosteal callus was defined as the callus inside this surface and intercortical callus as the callus existing between these two surface models. For each of these three zones, the mBMD and BV were measured.

**Statistical analysis.** The data on body weight, gap size and micro-CT evaluations of the BV and mBMD were analysed by one-way analysis of variance (ANOVA) using SPSS version 17.0 software (SPSS Inc., Chicago, Illinois). Homogeneity of variance was calculated using Levene statistics, according to which multiple pair-wise comparisons using a Tukey *post hoc* test were conducted to establish homogenous subsets and the Games-Howell *post hoc* test was used for unequal variance. Data on body weight and gap size were presented as the mean and SD and BV and mBMD data as the mean and the standard error of the mean (SEM). A *p*-value  $\leq 0.05$  was considered to be statistically significant.

## Results

**Body weight.** The mean body-weight of both the LIPUS and control groups on the day of operation and at every two weeks showed no significant differences for all groups at each time point (ANOVA, *p* = 0.55 on day at operation, *p* = 0.23 at two weeks, *p* = 0.17 at four weeks, *p* = 0.11 at six weeks and *p* = 0.55 at eight weeks) (Table I).

**Radiological.** The mean size of the gaps in each group is shown in Table II. No significant differences were apparent in any group at each time point (ANOVA, *p* = 0.74 on day of operation, *p* = 0.56 at two weeks, *p* = 0.48 at four weeks, *p* = 0.30 at six weeks and *p* = 0.65 at eight weeks).

**Micro-CT.** Typical images of the 3D reconstructed micro-CT scans at the ROI in the gap for both groups are shown in Figure 3. The mineralised areas of callus were larger in the LIPUS groups than in the control groups. The formation of cortex and medullary canal at the gap were more obvious in the LIPUS groups than in the control groups.

The mean volumetric BMD of mineralised tissue for each zone is shown in Figure 4. Within the control groups no significant differences were found at each interval. However, in the LIPUS groups, the mean mBMD was significantly higher at eight weeks than at four weeks for total, external, internal and endosteal zones (total,  $558.10 \text{ mg/cm}^3$  (SEM 16.32) *vs*  $332.52 \text{ mg/cm}^3$  (SEM 57.75); (*p* < 0.001); external,  $512.23 \text{ mg/cm}^3$  (SEM 12.88) *vs*  $307.65 \text{ mg/cm}^3$  (SEM 33.01) (ANOVA, *p* < 0.001); internal,  $508.22 \text{ mg/cm}^3$  (SEM 16.54), *vs*  $328.50 \text{ mg/cm}^3$  (SEM 40.44) (ANOVA, *p* < 0.001); endosteal,  $441.12 \text{ mg/cm}^3$  (SEM 19.18) *vs*  $313.13 \text{ mg/cm}^3$  (SEM 45.21) (*p* = 0.014)). Comparing the results at the same time points, between the two groups the mean mBMD was significantly higher at eight weeks in the LIPUS group than in the control group in both the external and intercortical zones.

The mean BV for each zone is shown in Figure 5. In the control group no significant differences were observed at each interval. However, in the LIPUS group, the mean BV

**Table I.** Details (kg, mean, SD) of the body-weight of both groups at each time interval

Group	Day of operation	Weeks			
		2	4	6	8
<b>4 weeks</b>					
Control	3.65 (0.22)	3.23 (0.25)	3.30 (0.26)		
LIPUS*	3.62 (0.25)	3.20 (0.22)	3.27 (0.31)		
<b>6 weeks</b>					
Control	3.73 (0.29)	3.49 (0.24)	3.47 (0.22)	3.46 (0.21)	
LIPUS	3.83 (0.19)	3.25 (0.13)	3.04 (0.04)	2.99 (0.29)	
<b>8 weeks</b>					
Control	3.47 (0.14)	3.06 (0.20)	3.12 (0.34)	3.14 (0.31)	3.08 (0.30)
LIPUS	3.58 (0.13)	3.05 (0.20)	3.23 (0.13)	3.20 (0.55)	3.18 (0.33)

\* LIPUS, low-intensity pulsed ultrasound stimulation

**Table II.** Details (mm, mean, SD) of the size of the osteotomy gap in both groups at each time interval

Group	Day of operation	Weeks			
		2	4	6	8
<b>4 weeks</b>					
Control	2.03 (0.05)	2.01 (0.07)	2.03 (0.12)		
LIPUS*	1.98 (0.08)	2.00 (0.08)	2.00 (0.12)		
<b>6 weeks</b>					
Control	1.99 (0.04)	1.98 (0.03)	1.98 (0.03)	2.00 (0.06)	
LIPUS	1.99 (0.02)	1.92 (0.05)	1.92 (0.05)	1.96 (0.08)	
<b>8 weeks</b>					
Control	2.08 (0.07)	2.06 (0.04)	1.94 (0.07)	2.02 (0.05)	2.00 (0.04)
LIPUS	2.03 (0.10)	2.08 (0.06)	2.05 (0.07)	2.01 (0.04)	2.02 (0.06)

\* LIPUS, low-intensity pulsed ultrasound stimulation

for the endosteal zone was significantly lower at eight weeks than at four weeks ( $0.13$ , SEM  $0.02 \times 10^{-2} \text{ cm}^3$  vs  $0.62$  SEM  $0.14 \times 10^{-2} \text{ cm}^3$ ,  $p = 0.02$ ).

Comparing the results at the same time point between the two groups, the mean BV in the intercorical zone at eight weeks was significantly higher in the LIPUS group than in the control group ( $1.37$  SEM  $0.13 \times 10^{-2} \text{ cm}^3$  vs  $0.37$  SEM  $0.15 \times 10^{-2} \text{ cm}^3$ , ANOVA,  $p < 0.001$ ).

## Discussion

In order to evaluate the effects of LIPUS using an animal model, it is desirable to adopt a method using a fracture with a sufficiently long healing process because osseous healing is usually so rapid that the effects of stimulation can barely be detected even when using sensitive methods of evaluation.<sup>2</sup> Secondly, since LIPUS is used clinically to encourage healing,<sup>17</sup> it is necessary to ensure that this approach is effective in stimulating retarded healing. In animal models, creating a model with sufficiently long healing is difficult.<sup>18,19</sup> We created a 2 mm gap at the site of the osteotomy<sup>20,21</sup> which was stabilised by a relatively stiff construct, as previously reported by mechanical testing.<sup>22</sup>

In previous studies, remodelling of callus has been evaluated histologically. In a rat fracture model it has been reported that woven bone is converted to lamellar bone at

the fracture site and that bone marrow is created in the remodelling stage.<sup>11</sup> Although histological examination is indispensable for observing the restructuring of woven bone from lamellar bone, the interpretation of the 3D callus structure from the 2D histological views is difficult.

One of the advantages of micro-CT is its higher resolution and the very thin slices which are scanned. Many slices can thus be obtained so that spatial differences within areas of the specimen become negligible. In addition, micro-CT allows automated acquisition and non-destructive morphological and densitometric assessments in 3D. In recent years, this technique has been used in many fields of orthopaedic research.<sup>9,10</sup> Using micro-CT, data on the geometrical properties of the healing bone can be acquired along with the spatial distribution of BMD by simultaneous scans of a calibration phantom. We selected the BV and the mBMD of the mineralised tissue comprising the callus volume as the denominator rather than tissue volume. The volume of callus represents the volume of mineralised tissue comprising the callus, but tissue volume includes the bone-marrow empty space around the callus. This means that the mBMD reflects the geometrical properties of the callus as well as density.

The availability of micro-CT for the evaluation of healing bones allows precise, 3D reconstruction of the callus

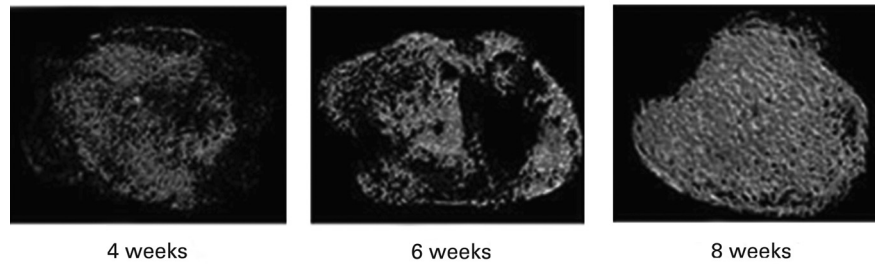


Fig. 3a

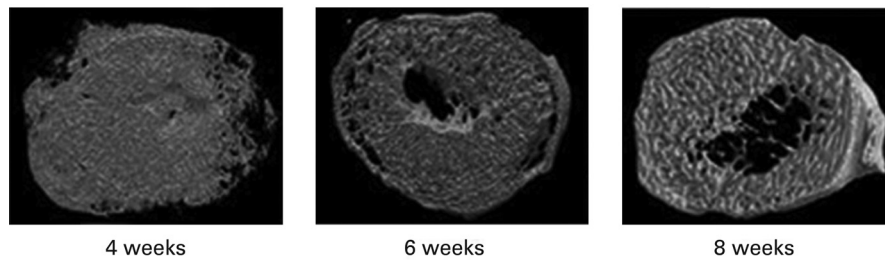


Fig. 3b

Three-dimensional micro-CT scans showing the region of interest in specimens from a) the control groups, with no evidence of the formation of either cortex or medullary canal, and b) the low-intensity pulsed ultrasound stimulation (LIPUS) groups, with an increase in both cortical area and medullary cavity observed over time.

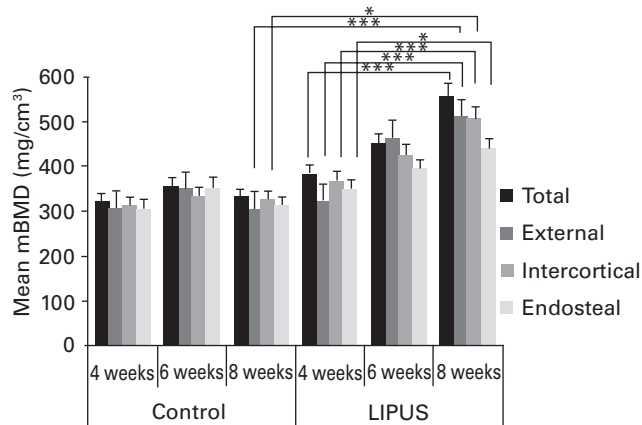


Fig. 4

Bar charts showing the volumetric bone mineral density (mBMD), presented as mean and SEM. In the low-intensity pulsed ultrasound stimulation (LIPUS) group, the mBMD was significantly higher in the eight-week group than in the four-week group in the total ( $p < 0.001$ ), external ( $p < 0.001$ ), intercortical ( $p < 0.001$ ) and endosteal zones ( $p = 0.014$ ). There was a significant difference between the eight-week control group and the eight-week LIPUS group in the external (\*\*\*,  $p = 0.14$ ) and intercortical (\*,  $p = 0.03$ ) zones.

and therefore evaluation of the true 3D callus volume and BMD. In both of these parameters, the optimum evaluation of quantitative changes in the localisation of regenerated callus can be performed.<sup>9</sup>

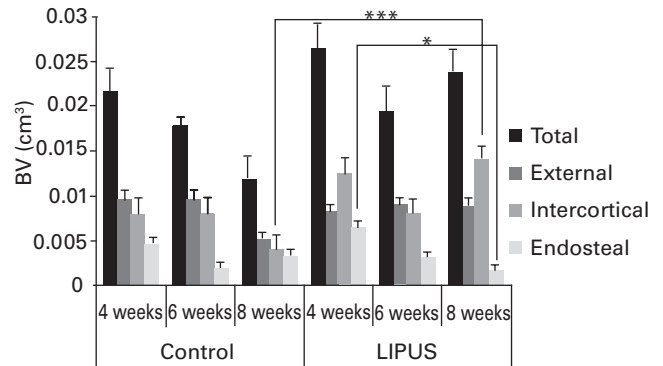


Fig. 5

Bar chart showing the results for callus volume (BV) with the mean and SEM. In the low-intensity pulsed ultrasound stimulation (LIPUS) groups, the BV for the endosteal zone was significantly lower for the eight-week group than for the four-week group (\*,  $p < 0.02$ ). Comparing the results at eight weeks, BV was significantly higher in the (LIPUS) groups than in the control groups for the intercortical zone (\*\*\*,  $p < 0.001$ ).

The mBMD in the endosteal area in the LIPUS group increased from four to eight weeks, whereas BV decreased during the same interval. In the endosteal area, this represented an increase in the density of newly-formed callus which was subsequently reduced by bone resorption that overwhelmed bone formation in this area. This remodelling process contributed to the formation of the medullary cav-

ity and appeared earlier in the LIPUS group, at eight weeks, than in the control group. In the control group, the remodelling process had not even started at eight weeks. In the intercortical area, the mBMD in the LIPUS group was significantly larger at eight weeks than in the same group at four weeks. Both the mBMD and BV in the intercortical area in the LIPUS group at eight weeks were larger than in the control group at eight weeks. LIPUS was thus considered to enhance bone formation in the intercortical area throughout that observation period. We expected bone resorption to occur after formation in the external area, but the mBMD in the LIPUS group was significantly larger at eight weeks than at four weeks. The BV at eight weeks in the LIPUS group, however, was no different from that at four weeks in the same group. This indicated that densification of the external area had occurred, in turn implying that LIPUS had the effect of increasing the rigidity and strength of the gap site, since the moment of inertia of the gap site could increase by this effect.

We observed corticalisation and formation of the medullary canal at the gap by examining changes in localisation of newly formed bone over time by measuring the volume of callus and the mBMD derived from micro-CT scans. In the late stage of fracture healing, resorption of external callus, corticalisation, and formation of the medullary canal took place at the healing site. This is the result of the remodelling of newly formed callus at the healing site. The process of healing was thought to differ between the periosteal and endosteal areas.

Our study focused on changes in the localisation of regenerated callus in a 3D plane under the effects of LIPUS. Subdividing the callus area into three zones was performed by using specially designed software. This method has not been described before, but was considered to be reproducible because the whole callus area was extracted using automated thresholding and the area measured by an automated counting technique.

The clinical relevance of our results is that these findings may contribute to determining the optimum timing of the initiation or duration of LIPUS. However, the most important issue in the enhancement of bone healing is to obtain earlier restoration of mechanical integrity in the healing bone. One of the limitations of our study was that we could not correlate the localisation of newly formed callus with mechanical integrity. Using micro-CT, data can be acquired on the structural and material properties of the healing bone by simultaneous scanning of a calibration phantom to obtain the spatial distribution of the BMD. From these data, strength-related parameters such as cross-sectional moment and cross-sectional moment of inertia at the healing site can be calculated. Basic *in vivo* animal studies have shown that these strength-related parameters from micro-CT correlate well with bending or torsional stiffness by mechanical testing.<sup>23,24</sup> Accordingly in future work we intend to evaluate the effects of LIPUS on the restoration of mechanical properties at the gap-healing site by analysing

strength-related parameters obtained from micro-CT scans and to relate these to data from mechanical testing.

In conclusion, LIPUS was found to be effective in accelerating healing in a rabbit tibial osteotomy with rigid fixation. It enhanced the formation of the medullary canal and cortex of the gap-healing model, which could lead to earlier restoration of the structural integrity of the healing site.

This project was supported by Teijin Pharma (Tokyo, Japan) which donated the LIPUS devices.

No benefits in any form have been received or will be received from a commercial party related directly or indirectly to the subject of this article.

## References

1. **Claes L, Willie B.** The enhancement of bone regeneration by ultrasound. *Prog Biophys Mol Biol* 2007;93:384-98.
2. **Pilla AA, Mont MA, Nasser PR, et al.** Non-invasive low-intensity pulsed ultrasound accelerates bone healing in the rabbit. *J Orthop Trauma* 1990;4:246-53.
3. **Yang KH, Parvizi J, Wang SJ, et al.** Exposure to low-intensity ultrasound increases aggrecan gene expression in a rat femur fracture model. *J Orthop Res* 1996;14:802-9.
4. **Rawool NM, Goldberg BB, Forsberg F, Winder AA, Hume E.** Power Doppler assessment of vascular changes during fracture treatment with low-intensity ultrasound. *J Ultrasound Med* 2003;22:145-53.
5. **Wang SJ, Lewallen DG, Bolander ME, et al.** Low intensity ultrasound treatment increases strength in a rat femoral fracture model. *J Orthop Res* 1994;12:40-7.
6. **Hantes ME, Mavrodontidis AN, Zalavras CG, et al.** Low-intensity transosseous ultrasound accelerates osteotomy healing in a sheep fracture model. *J Bone Joint Surg [Am]* 2004;86-A:2275-82.
7. **Christofolini L, Viceconti M.** Mechanical validation of whole bone composite tibia models. *J Biotech* 2000;33:279-88.
8. **Leung KS, Shi HF, Chung WH, et al.** Low magnitude high-frequency vibration accelerates callus formation, mineralization, and fracture healing in rats. *J Orthop Res* 2009;27:458-65.
9. **Nyman JS, Munoz S, Jadhav S, et al.** Quantitative measures of femoral fracture repair in rats derived by micro-computed tomography. *J Biomech* 2009;42:891-7.
10. **Freeman TA, Patel P, Parvizi J, Antoci V Jr, Shapiro IM.** Micro-CT analysis with multiple thresholds allows detection of bone formation and resorption during ultrasound-treated fracture healing. *J Orthop Res* 2009;27:673-9.
11. **Einhorn TA.** The cell and molecular biology of fracture healing. *Clin Orthop* 1998;355(Suppl):7-21.
12. **Azuma Y, Ito M, Harada Y, et al.** Low-intensity pulsed ultrasound accelerates rat femoral fracture healing by acting on the various cellular reactions in the fracture callus. *J Bone Miner Res* 2001;16:671-80.
13. **Chan CW, Qin L, Lee KM, et al.** Low intensity pulsed ultrasound accelerated bone remodelling during consolidation stage of distraction osteogenesis. *J Orthop Res* 2006;24:263-70.
14. **Augat P, Merk J, Genant HK, Claes L.** Quantitative assessment of experimental fracture repair by peripheral computed tomography. *Calcif Tissue Int* 1997;60:194-9.
15. **Malizos KN, Papachristos AA, Protopappas VC, et al.** Transosseous application of low-intensity ultrasound for the enhancement and monitoring of fracture healing process in a sheep osteotomy model. *Bone* 2006;38:530-9.
16. **Sing CC, Puh LH, Kumar AS.** Automatic hole repairing for cranioplasty using Bezier surface approximation. *J Craniofac Surg* 2005;16:1076-84.
17. **Jingushi S, Mizuno K, Matsushita T, Ibortan M.** Low-intensity pulsed ultrasound treatment for postoperative delayed union or nonunion of long bone fractures. *J Orthop Sci* 2007;12:35-41.
18. **Claes L, Augat P, Suger G, Wilke HJ.** Influence of size and stability of the osteotomy gap on the success of fracture healing. *J Orthop Res* 1997;15:577-84.
19. **Park SH, O'Connor K, Sung R, McKellop H, Sarmiento A.** Comparison of healing process in open osteotomy model and closed fracture model. *J Orthop Trauma* 1999;13:114-20.
20. **Carpenter JE, Hipp JA, Gerhart TN, et al.** Failure of growth hormone to alter the biomechanics of fracture-healing in a rabbit model. *J Bone Joint Surg [Am]* 1992;74-A:359-67.
21. **Park SH, Silva M.** Effect of intermittent pneumatic soft-tissue compression on fracture-healing in an animal model. *J Bone Joint Surg [Am]* 2003;85-A:1446-53.
22. **Gilley RS, Beason DP, Snyder M, et al.** External fixator clamp reuse degrades clamp mechanical performance. *Vet Surg* 2009;38:530-6.
23. **Jamsa T, Jalovaara P, Peng Z, Väänänen HK, Tuukkanen J.** Comparison of three-point bending test and peripheral quantitative computed tomography analysis in the evaluation of the strength of mouse femur and tibia. *Bone* 1998;23:155-61.
24. **Lind PM, Lind L, Larsson S, Orberg J.** Torsional testing and peripheral quantitative computed tomography in rat humerus. *Bone* 2001;29:265-70.